Journal of Gerontology: BIOLOGICAL SCIENCES
2008, Vol. 63A, No. 12, 1267–1276

Age-Related Markers Assayed at Different Developmental Stages of the Annual Fish *Nothobranchius rachovii*

Chin-Yuan Hsu,[1,2,3] Ya-Chi Chiu,[2] Wei-Lun Hsu,[1] and Yu-Pei Chan[2]

[1]Department of Life Science, [2]Graduate Institute of Basic Medical Science, and
[3]Center for Healthy Aging Research, Chang Gung University, Tao-Yuan, Taiwan.

Although short-lived vertebrates can serve as model animals for understanding the mechanism of aging, whether the annual fish *Nothobranchius rachovii* is suitable for studying aging remains an open question. In this study, histochemical, biochemical, and genetic techniques were used to determine the age-related markers at three different developmental stages of the annual fish *N. rachovii*. Histochemical studies revealed that the expression of senescence-associated β-galactosidase and accumulation of lipofuscin increased with age. In biochemical assays, lipid peroxidation and protein oxidation increased with age, whereas the activities of catalase, glutathione peroxidase, and superoxide dismutase decreased with age. Genetic analysis established that the activities of telomerase had no apparent relationship with age, but telomere lengths reduced with age from 11.5 ± 1.98 to 3.58 ± 0.74 kb. Taken together, these results indicate that the annual fish *N. rachovii* may be useful as an animal model for the study of aging.

Key Words: Aging—Lipofuscin—Lipid oxidation—Protein oxidation—Catalase—Glutathione peroxidase—Superoxide dismutase—Telomerase—Telomere length—*Nothobranchius rachovii*.

UNDERSTANDING the biology of aging has become one of the major scientific challenges in the quest to prevent and cure age-associated diseases, such as cardiovascular disease, cancer, arthritis, cataracts, osteoporosis, type 2 diabetes, and Alzheimer's disease (1–3). Numerous model organisms have been used to study senescence, including yeast (*Saccharomyces cerevisiae*) (4), worm (*Caenorhabditis elegans*) (5), fruit fly (*Drosophila melanogaster*) (6), zebrafish (*Danio rerio*) (7–10), mouse (11), rat (12), dog (13), and sheep (14). Nevertheless, a model vertebrate animal with a shorter life span and an aging process similar to that of human beings has not been established.

Fish appear to be useful as a potential animal model for the study of aging (15–17). Zebrafish have been used to study vertebrate development, neurobiology, and genetics (18) because of some of their attributes, such as the conservation of the developmental genes observed across vertebrates, morphological and physiological similarities to mammals, and the ease of administration of water-soluble drugs and chemicals (7,19,20). Zebrafish have also been used to study aging (8–10). However, the mean life span of zebrafish is approximately 3.5 years, and the maximum life span is about 5 years (7). In contrast, annual fish—*Cynolebias adloffi*, *Nothobranchius guentheri*, *N. furzeri*, and *N. rachovii*—have been proposed as an alternative model animal for the study of aging (21–25). *N. furzeri* have a relatively short life span (3 months), and are suspected to have accelerated aging, sudden-death syndrome, and vulnerable to the velvet disease (26). However, the annual fish *N. rachovii* were also reported to have a relatively short life span (8.5 months), which is quite shorter than that of other species, and may be suitable for the study of aging (24).

The aim of the present study is to evaluate the changes in the expression of age-related markers during the aging process in the annual fish *N. rachovii* and to determine its suitability as a model animal for the study of aging. We used histochemical techniques to examine the expression of senescence-associated β-galactosidase (SA-β-Gal) (27) and accumulation of lipofuscin (28). We also examined protein oxidation (29), lipid peroxidation (30), and the activities of catalase (CAT), glutathione peroxidase (GPX), and superoxide dismutase (SOD) (31,32) by biochemical techniques, as well as the activity of telomerase (33) and telomere length (34). These markers were assessed at three different developmental stages (at 1, 4, and 7 months of age) of the annual fish *N. rachovii*.

Methods

The Annual Fish

Male *N. rachovii* about 1, 4, and 7 months old were purchased from Taikong Group (Taipei, Taiwan), temporarily maintained (at five fishes per 9 L tank) on a 14-hour light/10-hour dark cycle with low flow rate at 26 ± 1°C for 1 week and with artificial plants for the fish to settle in. Live brine shrimp were fed to the fish twice per day, and flake food was occasionally given. Ultraviolet (UV) lamps were

used to disinfect water to prevent the spread of disease in the recirculating system. Water pH was maintained at 7.0 ± 0.2. Water ammonia, nitrate, and nitrite are maintained at 25 ± 8.6, 0.04 ± 0.01, and 0, respectively. The health of each fish was observed daily. The healthy fishes were used for this study. All males were killed at 4°C before carrying out the following experiments.

SA-β-Gal staining

The gills were freshly dissected from fishes, fixed for 1 hour in 3% formaldehyde at room temperature, washed in phosphate-buffered saline (PBS), frozen at −80°C, and mounted in optimal cutting temperature (OCT) compound. Thin sections (8 μm) were cut at −20°C with a cryosectioning system (CM 3050S; Leica [Chang Gung University]), mounted onto glass slides, immersed overnight in SA-β-Gal stain solution (27), counterstained with eosin, and viewed under bright field. Gill epithelia were analyzed with five age-matched fishes per age. The area and intensity of expression of SA-β-Gal were analyzed with ImageJ software (http://rsb.info.nih.gov/ij).

Lipofuscin Staining

Lipofuscin in the sections of gills were observed by fluorescence light microscopy (35). Autofluorescence of lipofuscin granules were evaluated with blue (450–490 nm) excitation light, with 520-nm emission filters, respectively (9). Gill epithelia were analyzed with five age-matched fishes per age. The intensity of lipofuscin was analyzed with ImageJ software (http://rsb.info.nih.gov/ij).

Assay for Lipid Peroxidation

Estimates of lipid peroxidation levels were evaluated by the thiobarbituric acid reactive substances (TBARS) procedure (36). The body from pectoral fin to tail fin containing only skin, bones, red and white muscle, excluding head and internal organs, was as the resource of material. Briefly, 1 g of material was homogenized in 5 mL of 50 mM phosphate buffer (pH 7.5) by using a polytron and sonicator. The homogenate was centrifuged at 5000 × *g* for 10 minutes. The resulting supernatant (0.5 mL) was mixed with 2.5 mL of trichloroacetic acid solution (at 100 μg/mL) in a test tube, and the mixture was heated at 95°C for 15 minutes. After cooling in tap water, the tube was centrifuged at 1000 × *g* for 10 minutes, and 2 mL of the supernatant was added to 1 mL of thiobarbituric acid (TBA) solution at 6.7 mg/mL in a test tube. The tube was then placed in a boiling water bath for 15 minutes. The solution was then cooled in tap water, and its absorbance was measured using a spectrophotometer at 532 nm. The concentration of malondialdehyde (MDA) was calculated by the absorbance coefficient of the MDA–TBA complex (absorbance coefficient = 1.56×10^5 cm^{-1} M^{-1}) and is expressed as nanomoles per gram of protein (37). The protein content of the supernatant was determined by using the Lowry method (38).

Assay for Protein Oxidation

Protein carbonyls in materials were determined by using a spectrometric 2,4-dinitrophenylhydrazones (DNPH) assay with a minor modification (39). Briefly, 1 g of material was homogenized in 5 mL 50 mM phosphate buffer (pH 7.5) containing protease inhibitors (leupeptin at 0.5 μg/mL, aprotinin at 0.5 μg/mL, pepstatin at 0.7 μg/mL, phenylmethylsulfonyl fluoride [PMSF] at 40 μg/mL) by using a polytron and sonicator. The homogenate was centrifuged at 5000 × *g* for 10 minutes. The protein content of the supernatant was determined by using the Lowry method (38). From the resulting supernatant, 300-μL aliquots containing 1.7–2.5 mg of protein were treated with 300 μL of 10 mM DNPH dissolved in 2 M HCl or with 2 M HCl in the controls. Materials were then incubated for 1 hour at room temperature, stirred every 10 minutes, precipitated with 10% trichloroacetic acid (final concentration), and centrifuged at 7800 × *g* for 3 minutes. The pellet was washed thrice with 1 mL of ethanol/ethyl acetate, 1:1 (vol/vol) and redissolved in 1 mL of 6 M guanidine in 10 mM phosphate buffer/trifluoroacetic acid, pH 2.3. Any trace insoluble material was removed by centrifugation at 7800 × *g* for 3 minutes. The difference in absorbance between the DNPH- and HCl-treated material was determined at 366 nm, and the results were expressed as nanomoles of carbonyl groups per milligram of protein, using the extinction coefficient of 22.0 $mM^{-1}cm^{-1}$ for aliphatic hydrazones (40).

Assay for CAT Activity

The CAT assay was carried out by the method of Yen with slight modifications (41). Briefly, 1 g of material was homogenized in 5 mL of 50 mM phosphate buffer (pH 7.0) by using a polytron and sonicator. The homogenate was centrifuged at 5000 × *g* for 10 minutes. The assay reaction consisted of 50 mM potassium phosphate buffer (pH 7.0), 100 μL of 30% H_2O_2, and the resulting supernatant in a total volume of 1 mL. The reaction was carried out at 25°C. Blank control was prepared with 900 μL of 50 mM potassium phosphate buffer and 100 μL of 30% H_2O_2. The rate of absorbance change ($\triangle A$/min) at 240 nm was recorded, which indicated the decomposition of H_2O_2. Activities were calculated by using the molar extinction coefficient of H_2O_2 at 240 nm, 43.59 L/mol/cm. Units of CAT were expressed as the amount of enzyme that decomposes 1 μmol of H_2O_2 per minute at 25°C. The specific activity was expressed in terms of micromoles per minute per milligram of protein.

Assay for GPX Activity

GPX activity was assayed with a coupled enzyme system in which oxidized glutathione (GSSG) reduction was coupled to NADPH oxidation by glutathione reductase following a previously described method (41,42) with modification. Briefly, 1 g of material was homogenized in 5 mL of 50 mM Tris-HCl buffer (pH 7.6) containing protease inhibitors (leupeptin at 0.5 μg/mL, aprotinin at 0.5 μg/mL, pepstatin at 0.7 μg/mL, PMSF at 40 μg/mL) by using a polytron and sonicator. The homogenate was centrifuged at 5000 × *g* for 10 minutes. The coupling reagent contained 50 mM Tris-HCl (pH 7.6), 2 mM EDTA, 1 mM NaN_3, 1 mM reduced glutathione (GSH), 0.2 mM NADPH, and 100 U glutathione reductase. Supernatant diluted in Tris-HCl buffer in the volume of 100 μL was preincubated with 875 μL of the coupling reagent for

2 minutes at 25°C, and the reaction was initiated by the addition of 25 μL of H_2O_2 at the final concentration of 25 μM. The decrease in the absorbance at 340 nm was followed spectrophotometrically.

Assay for SOD activity

The assay of SOD was based on the reduction of nitroblue tetrazolium (NBT) to water-insoluble blue formazan (43). Briefly, 1 g of material was homogenized in 5 mL of 50 mM phosphate buffer (pH 7.8) by using a polytron and sonicator. In a final 1 mL reaction, the final concentration of reaction mixture contained 50 mM phosphate buffer (pH 7.8), 1 mM diethylenetriaminepentaacetic acid (DETAPAC), 1 U CAT, 5.6 μM NBT, 0.1 mM xanthine, 50 mM bathocuproine sulfonate (CBCS), and an appropriate amount of xanthine oxidase for obtaining the required reference rate. The rate of NBT reduction was monitored at 560 nm at 25°C. Xanthine oxidase was diluted to the point that the blank rate without material was between 0.02 and 0.05 optical density. Eight reactions with different dilutions of the same material were carried out. One unit of SOD was defined as the amount of protein that resulted in 50% inhibition of the rate of NBT reduction. When 5 mM sodium cyanide was included in the mixture, activity of Mn-SOD was measured; otherwise, the activity of total SOD was obtained. The activity of Cu, Zn-SOD was calculated by subtracting Mn-SOD activity from total SOD activity.

Assay for Telomerase Activity

Telomerase activity was measured with the telomere repeat amplification protocol (TRAP) by using the TRAPeze kit. Briefly, 100 mg of material treated with 200 μL of ice-cold lysis buffer (0.5% 3-[(3-cholamidopropyl)-dimethylammonio]-1-propane sulfonate [CHAPS], 10 mM Tris-HCl [pH 7.5], 1 mM $MgCl_2$, 1 mM EGTA, 10% glycerol, 5 mM β-mercaptoethanol, and 1 mM PMSF), then incubated on ice for 30 minutes. After centrifugation at 15,000 × *g* for 30 minutes at 4°C, DNA concentration in supernatant was measured by UV absorbance before it was stored at −80°C. One microliter of the extension products of telomerase were amplified by a three-step polymerase chain reaction (PCR; 94°C for 30 seconds, 52°C for 30 seconds, 72°C for 30 seconds) for 29 cycles of PCR in the presence of a TS primer and resolved on 10% polyacrylamide gel. Telomerase was quantified by normalizing the band intensities of the characteristic every 6-bp telomerase-specific ladder band by using ImageJ software (44).

Assay for Telomere Length

Telomere length analysis was performed by Southern blot hybridization using the telomere length kit (Roche, Germany). Briefly, high-molecular-weight genomic DNA was isolated from the material that was digested with proteinase K in lysis buffer (10 mM Tris-HCl, 100 mM NaCl, 100 mM EDTA, 0.5% sodium dodecyl sulfate [SDS], and RNase at 0.1 mg/mL), extracted with isopropanol–ethanol, and verified by standard agarose gel electrophoresis. Two micrograms of genomic DNA was digested with *Hinf*I and *Rsa*I enzymes at 37°C for 3 hours and subjected to 0.8% agarose gel electrophoresis for 4 hours at 75 V. Digested DNA was then transferred to Hybond N^+/nylon membrane. A DIG-labeled oligonucleotide probe $(CCCTAA)_3$ was hybridized to the membrane and detected using enhanced chemiluminescent detection (TeloTAGGG telomere length assay). Telomere lengths were analyzed by using ImageQuant software (Chang Gung University). All materials were analyzed with five age-matched fishes per age, and the results were averaged (45).

Statistical Analysis

The differences among three age groups were examined by using one-way analysis of variance. The Tukey's Honestly Significant Differences (HSD) test is then used for pairwise comparisons. A value of $p < .05$ is considered statistically significant.

Results

Male Fish of 1-, 4-, and 7-Month-Old Stages

The healthy males were selected for study and evaluated by motion, appetite, and exterior pathological changes. The average size of male fish at the 1-, 4-, and 7-month-old stages is 2.3 ± 0.15 cm in length and 0.4 ± 0.08 cm in width, 3.7 ± 0.22 cm in length and 0.8 ± 0.11 cm in width, and 4.3 ± 0.35 cm in length and 1.2 ± 0.15 cm in width, respectively (Figure 1A–D). The morphology of body illustrates that fish grows with age.

Histochemical Examination of SA-β-Gal and Lipofuscin Granules

SA-β-Gal in the cells stains blue with X-gal. The more prevalent the blue color, the higher the SA-β-Gal expression. The blue color observed in gill epithelium was faint at the 1-month-old stage (Figure 2A), but was observed to have increased at the 4- and 7-month-old stages (Figure 2B and C). The gill epithelia at 7 months exhibited a darker blue color than did those at 4 months. The results revealed that not only did SA-β-Gal-containing stained cell area, but also its color intensity, increased with age ($p < .001$) (Figure 2D and E). This result indicates that the accumulation of SA-β-Gal increased with age in the *N. rachovii*.

Lipofuscin appears as bright-green-colored dots in the cells. The gill epithelium exhibited only a few bright-green-colored dots at the 1-month-old stage (Figure 3A), but the number of dots were observed to have increased at the 4- and 7-month-old stages (Figure 3B and C). The gill epithelium at 7 months exhibited brighter green-colored dots than those at 4 months ($p < .001$) (Figure 3D). These results show that, similar to SA-β-Gal, the accumulation of lipofuscin increased with age in the annual fish *N. rachovii*.

Protein Oxidation and Lipid Peroxidation Analyses

Next, levels of protein oxidation were assessed by determining the carbonyl contents of amino acids derived by using DNPH. The mean values obtained for carbonyl-group content were 2.78 ± 0.65, 3.73 ± 0.18, and 4.48 ± 0.23 nmol/mg protein at the 1-, 4-, and 7-month-old stages, respectively ($p < .001$) (Figure 4A). The carbonyl-group content was observed to increase with the progression of

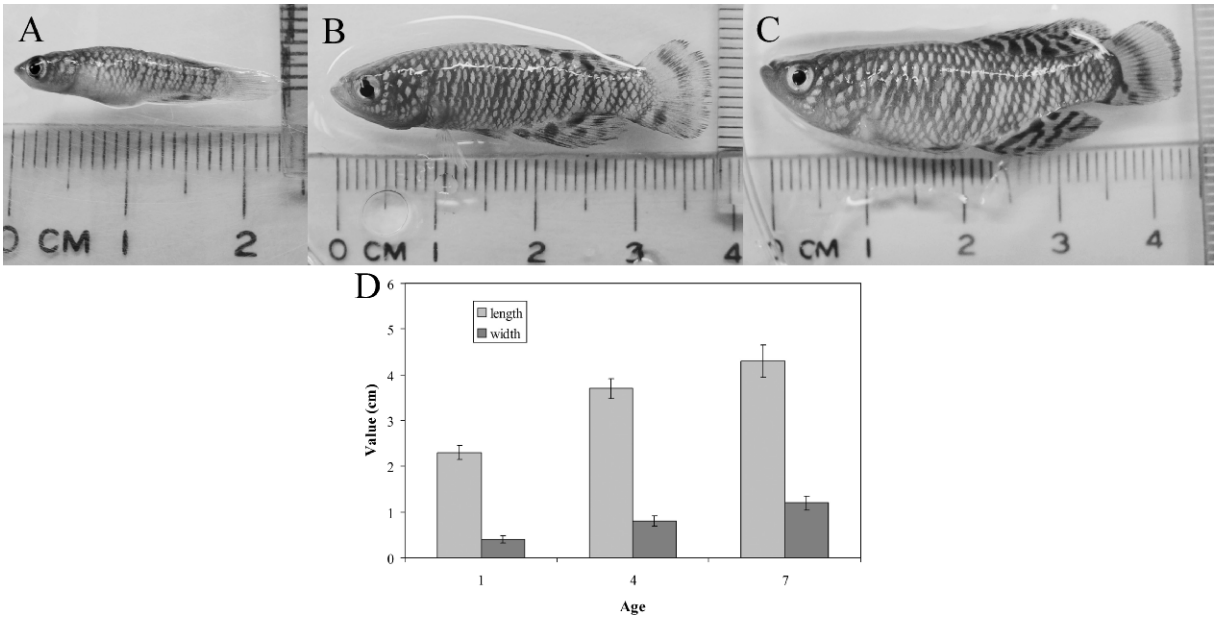

Figure 1. *Nothobranchius rachovii* at the 1-, 4-, and 7-month-old stages. **A,** Male *N. rachovii* at 1 month old. **B,** Male *N. rachovii* at 4 months old. **C,** Male *N. rachovii* at 7 months old. **D,** Average length and width of body in male fish at the 1-, 4-, and 7-month-old stages.

developmental stages, thus indicating an age-dependent elevation in protein oxidation in the annual fish *N. rachovii*.

In addition, lipid peroxidation was assessed by determining the levels of MDA, a metabolite of lipid peroxidation. The mean values obtained for MDA were 1.96 ± 0.30, 4.76 ± 0.41, and 6.74 ± 0.98 nmol/mg protein at the 1-, 4-, and 7-month-old stages, respectively ($p < .001$) (Figure 4B). The levels of MDA increased with the progression of developmental stage. This result displays that lipid peroxidation increased with age in *N. rachovii*.

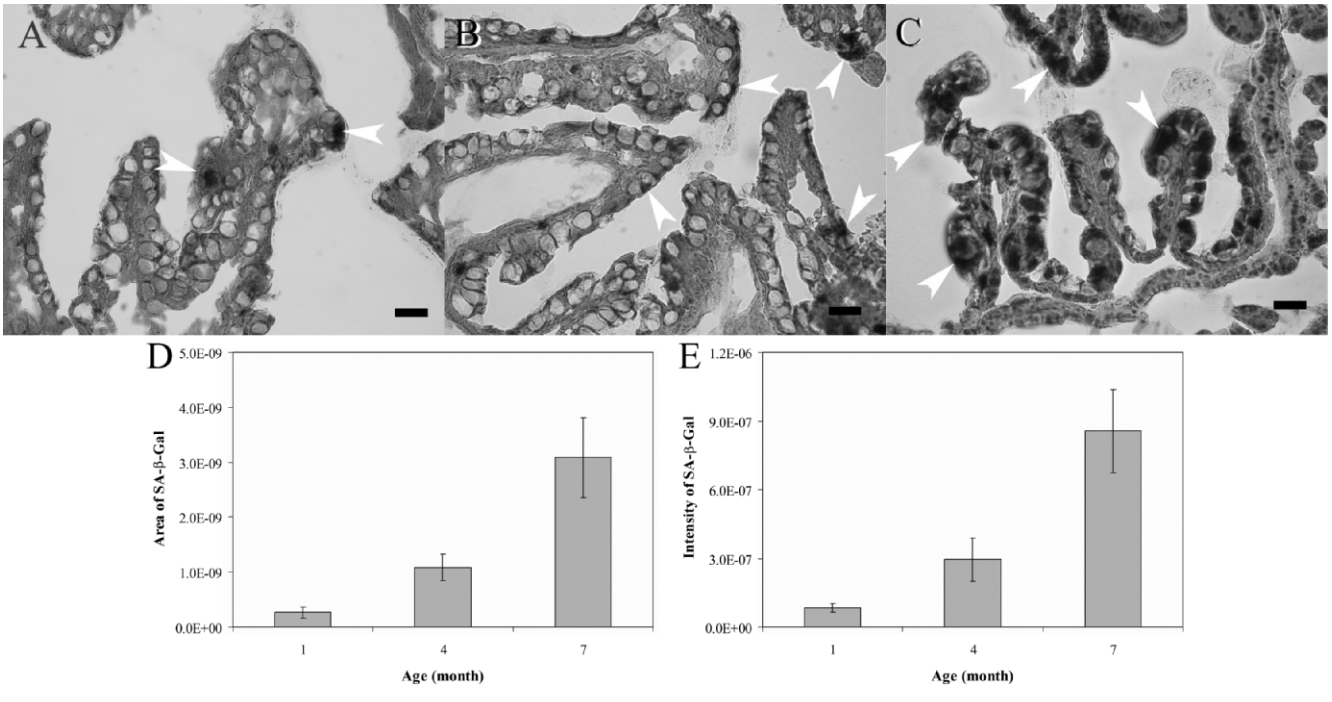

Figure 2. Senescence-associated β-galactosidase (SA-β-Gal) in gill epithelium at the 1-, 4-, and 7-month-old stages. **A,** Small amount of SA-β-Gal accumulation at 1 month. *Arrow head* shows area of SA-β-Gal staining. Scale bar = 10 μm. **B,** Increase in SA-β-Gal accumulation at 4 months. *Arrow head* shows the area of SA-β-Gal staining. Scale bar = 10 μm. **C,** Further increase in SA-β-Gal accumulation at 7 months. *Arrow head* shows the area of SA-β-Gal staining. Scale bar = 10 μm. **D,** Area of SA-β-Gal in stained gill epithelium. Data represent mean ± standard deviation (*SD*) ($N = 5$). **E,** Intensity of SA-β-Gal in stained gill epithelium. Data represent mean ± *SD* ($N = 5$).

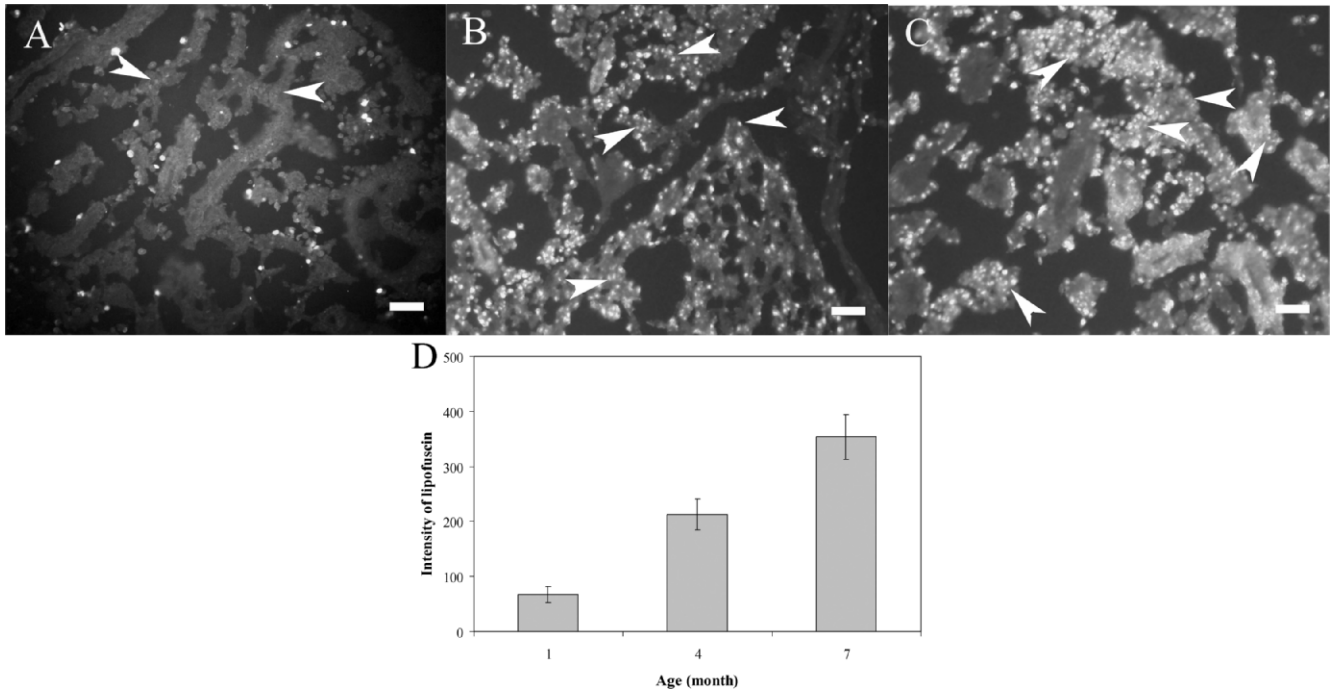

Figure 3. Lipofuscin in gill epithelium at 1-, 4-, and 7-month-old stages. **A,** Accumulation of only a few lipofuscin at 1 month. *Arrow head* shows lipofuscin granules. Scale bar = 25 μm. **B,** Increase in the accumulation of lipofuscin at 4 months. *Arrow head* shows lipofuscin granules. Scale bar = 25 μm. **C,** Further increase in the accumulation of lipofuscin at 7 months. *Arrow head* shows lipofuscin granules. Scale bar = 25 μm. **D,** Number of lipofuscin granules in stained gill epithelium. Data represent mean ± standard deviation ($N = 5$).

Determination of the Activities of CAT, GPX, and SOD

Figure 5A illustrates the results from the CAT activity. The mean values obtained for CAT activity were 28.95 ± 1.13, 16.54 ± 0.9, and 7.66 ± 0.18 μmol/min/mg protein at the 1-, 4-, and 7-month-old stages, respectively ($p < .001$). Figure 5B shows the GPX activity. The mean values obtained for the GPX activity were 23.57 ± 1.65, 15.32 ± 0.67, and 10.14 ± 0.54 nmol/min/mg protein at the 1-, 4-, and 7-month-old stages, respectively ($p < .001$). Figure 5C represents the results of the Mn-SOD activity. The mean values obtained for Mn-SOD activity were 13.03 ± 2.51, 8.22 ± 0.95, and 6.9 ± 0.19 U/mg protein at 1-, 4-, and 7-month-old stages, respectively ($p < .001$). Additionally, the mean values obtained for Cu, Zn-SOD activity were 58.81 ± 2.52, 32.23 ± 0.64, and 24.97 ± 4.01 U/mg protein at the 1-, 4-, and 7-month-old stages, respectively ($p < .001$), as shown in Figure 5D. These results collectively demonstrate that the activities of CAT, GPX, Mn-SOD, and Cu, Zn-SOD decreased with the age in *N. rachovii*.

Determination of Telomerase Activity and Telomere Length

To further determine the progressive aging processes of the annual fish, the activities of telomerase and telomere length were determined. Telomerase activity was found to have no apparent relationship with age in *N. rachovii*. This conclusion was reached after monitoring the *N. rachovii*

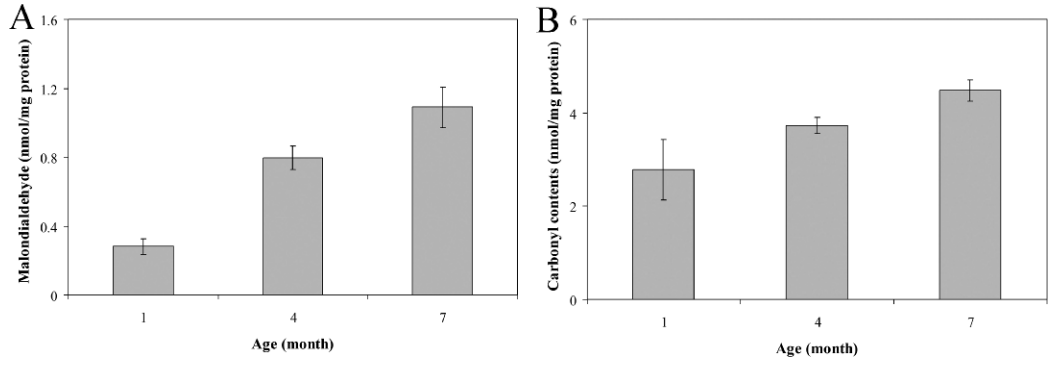

Figure 4. Lipid peroxidation and protein oxidation at the 1-, 4-, and 7-month-old stages. **A,** Lipid peroxidation levels. Data represent mean ± standard deviation (*SD*) ($N = 5$). **B,** Protein oxidation levels. Data represent mean ± *SD* ($N = 5$).

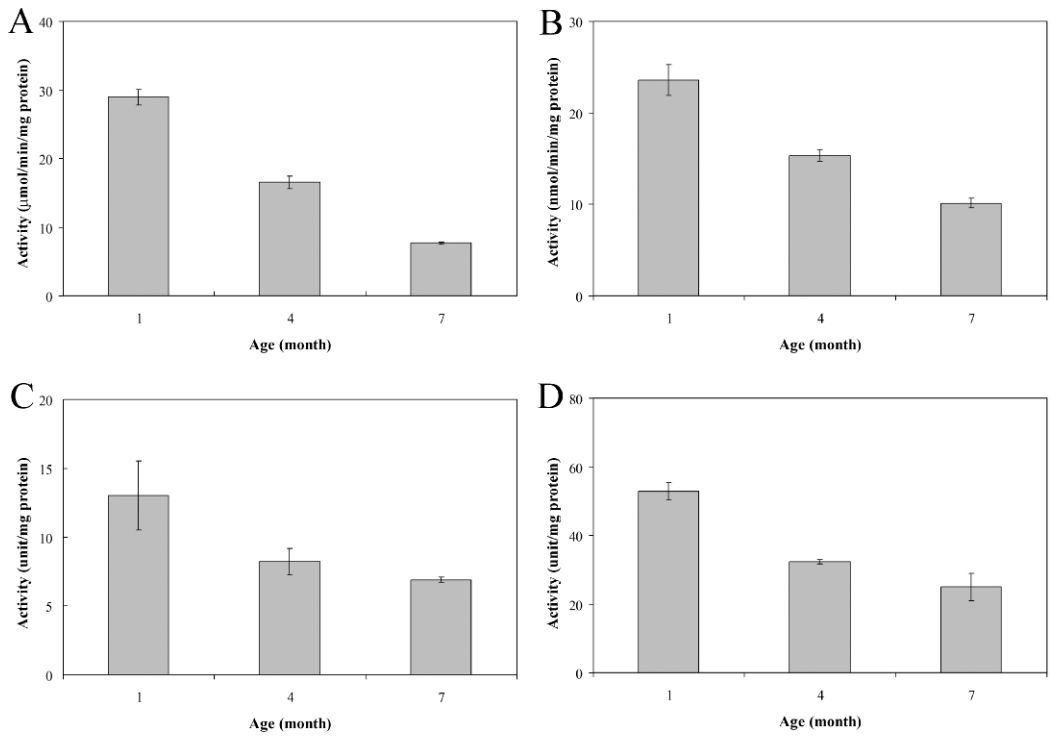

Figure 5. The activities of catalase (CAT), glutathione peroxidase (GPX), Mn-superoxide dismutase (Mn-SOD), and Cu, Zn-SOD at the 1-, 4-, and 7-month-old stages. **A,** CAT activity. Data represent mean ± standard deviation (*SD*) ($N = 5$). **B,** GPX activity. Data represent mean ± *SD* ($N = 5$). **C,** Mn-SOD activity. Data represent mean ± *SD* ($N = 5$). **D,** Cu, Zn-SOD activity. Data represent mean ± *SD* ($N = 5$).

developmental stages (Figure 6A), and was further verified by statistical analysis ($p < .001$) (Figure 6D). To study the telomere length of *N. rachovii*, we isolated its genomic DNA (Figure 6B) and found that the telomere length shortened with the progression of developmental stages (Figure 6C). The average telomere length was determined to be approximately 7.31 ± 0.73, 6.56 ± 0.36, and 5.18 ± 0.28 kb at the 1-, 4-, and 7-month-old stages, respectively ($p < .001$) (Figure 6E). The average telomere lengths ranged from 3.58 ± 0.74 to 11.5 ± 1.98 kb. These results imply that telomerase activity had no apparent relationship with age, whereas the telomere length shortened with age. Taken together, the above-mentioned results further indicate that these aging markers increase with age in *N. rachovii*.

Discussion

In this study, we discovered that the expression of SA-β-Gal, accumulation of lipofuscin, lipid peroxidation, and protein oxidation increased with age, and that activities of CAT, GPX, and SOD decreased with age. Whereas the telomerase activity did not undergo a change with age, the telomere lengths shortened with age. These data strongly suggest that the annual fish *N. rachovii* may be useful as an animal model for the study of aging.

Histochemical Examination of SA-β-Gal and Lipofuscin

SA-β-Gal is a eukaryotic hydrolase localized in the lysosome and can accumulate with age (46). SA-β-Gal has been broadly used to examine the cellular aging process of many adult somatic tissues and cultured cells in different animal models (9,27,47). In the case of studies conducted on fish, SA-β-Gal was confirmed to be related to aging in the skin and dermis of zebrafish (*Danio rerio*) (9) as well as the annual fish *N. furzeri* (47,48). In this study, the expression of SA-β-Gal in gill epithelium was related to the aging of annual fish *N. rachovii*, thus our findings correlated with those in studies of zebrafish (9) and *N. furzeri* (47,48).

Lipofuscin is an intralysosomal polymeric material and originates from autophagocytosed cellular components oxidized outside or inside the lysosomal compartment (49); it can be neither degraded by lysosomal hydrolases, nor exocytosed. Lipofuscin accumulates with age and has been extensively used to examine the cellular aging process of many adult somatic tissues and cells in different animal models (9,28,35,47,50). Lipofuscin has been confirmed to be related to aging in the muscle of zebrafish (*Danio rerio*) (9) and in the liver and caudal peduncle of annual fish *N. furzeri* (47,48). In this study, the expression of lipofuscin in gill epithelium was observed to be related to the aging of *N. rachovii*; this finding is consistent with those in studies of zebrafish (9) and *N. furzeri* (47,48).

We use gills to study the expression of SA-β-Gal and accumulation of lipofuscin because gills are in contact with the outside environment. By studying the response of gill epithelium, we may understand the effects of stresses on aging. However, the small size of the gills limits its use; therefore, we use the body (after the removal of head and internal organs) as the source of material for protein

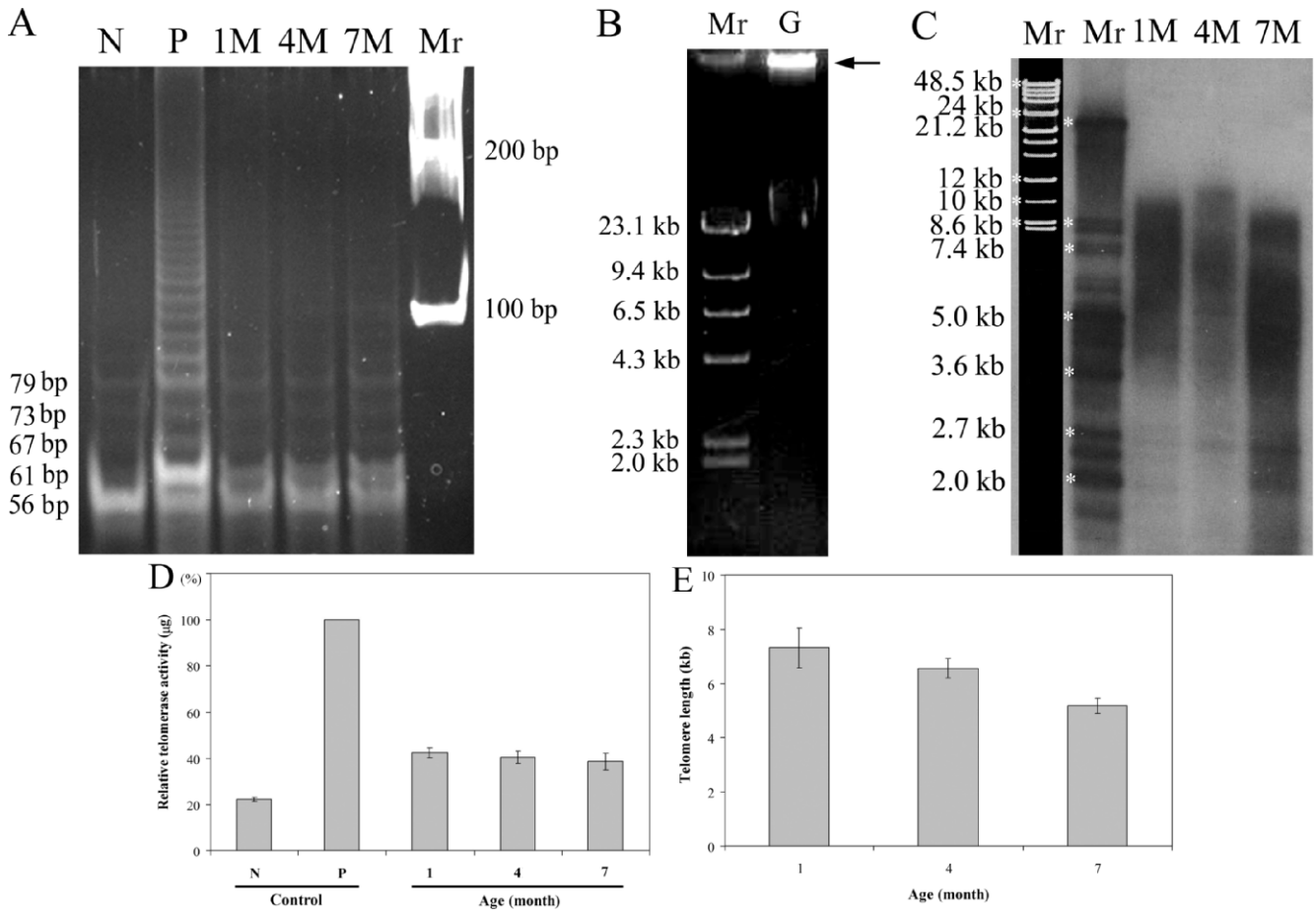

Figure 6. Telomerase activity, genomic DNA, and telomere length at the 1-, 4-, and 7-month-old stages. **A,** Telomerase activity. N: negative control; P: positive control; 1M: 1 month old; 4M: 4 months old; 7M: 7 months old; Mr: markers. **B,** Genomic DNA. *Arrow* shows genomic DNA. Mr: markers; G: genomic DNA. **C,** Telomere length. Mr: markers; 1M: 1 month old; 4M: 4 months old; 7M: 7 months old. *Markers' lengths derived from markers' bands. **D,** Quantification of telomerase activity. Positive control represents 100% telomerase activity. N: negative control; P: positive control. Data represent mean ± standard deviation (*SD*) ($N = 5$). **E,** Quantification of telomere length. Data represent mean ± *SD* ($N = 5$).

oxidation, lipid peroxidation, enzyme activities, and telomere length assays.

Protein Oxidation and Lipid Peroxidation Analyses

Lipid peroxidation and protein oxidation, induced by reactive oxygen species (ROS), have been found to increase with age in many adult somatic tissues and cells in different animal models (30,40,51,52). Hence, protein oxidation and lipid peroxidation are often considered as the index of aging. For monitoring protein oxidation, carbonyl groups are the general marker (39,53), whereas MDA is examined for lipid peroxidation (36). The levels of lipid peroxidation and protein oxidation were found to increase with age in *N. rachovii*, consistent with the results of previous studies in other species (30,40,51,52). Previous studies showed that protein carbonylation can be produced by ROS, oxidative cleavage of proteins, and lipid-derived aldehydes including MDA, acrolein, 4-hydroxy-*trans*-2-nonenal, glyoxal, 4-oxo-*trans*-2-nonenal, levuglandin E2, and levuglandin D2 (54–56). Also, protein carbonylation formed from lipid-derived aldehydes is more prevalent than that formed via direct amino acid side chain oxidation (57). Therefore, greater incremental increase occurs in the first three months of age in MDA measurements as compared to protein carbonyls.

Furthermore, the incremental increase in accumulated oxidative damage in above-mentioned molecules may reflect age-related declines in the efficiency of degradation and repair processes (58–61) and/or a gradual accumulation of damage in tissues with low turnover (62,63).

Determination of the Activities of CAT, GPX, and SOD

ROS—resulting in lipid peroxidation, protein oxidation, and DNA damage—can be scavenged by antioxidant enzymes such as CAT, GPX, Mn-SOD, and Cu, Zn-SOD (64). The activities of CAT, GPX, and SOD have been reported to decrease with age in many adult somatic tissues and cells in different animal models (65–69). The down-regulated activities of CAT, GPX, and SOD with age in *N. rachovii* are consistent with the results of previous studies in other species (65–69). The age-related decline in antioxidant

levels most likely is not a result of lower ROS production, because ROS usually increases with age (70). The reason for the decline of antioxidant levels may be the impairment of antioxidant enzymes (71) or down-regulation of antioxidant enzymes (72).

Determination of Telomerase Activity and Telomere Length

Telomerase is a ribonucleoprotein reverse transcriptase capable of synthesizing terminal TTAGGG telomeric repeats at the ends of chromosomes (73). Telomerase activity is repressed or decreases with age in many adult somatic tissues and cultured cells in different animal models (14,74). This absence of telomerase activity is correlated with telomeric shortening that occurs with age in vivo and in vitro (13,45). Among fishes, telomerase activity has been studied in zebrafish, pufferfish (*Fugu rubripes*), and medaka (*Oryzias melastigma*) (9,75–77); only in zebrafish was it studied in the context of aging. However, it exhibited no apparent relationship with age. Our study on *N. rachovii* also yielded the same result.

Telomeres are specialized DNA–protein complexes that cap the ends of linear chromosomes, consisting of simple repetitive DNA that in mammals comprise (TTAGGG)n (64), and shorten progressively with cell division (12,78–80). Telomere shortening may result in cell senescence as observed in many adult somatic tissues and cells in different animal models (12–14,45,81). This study shows that telomeres shorten with age in *N. rachovii*, and is consistent with those of previous studies in other species (12–14,45,81). The telomere lengths of different species have been determined in mammals and nonmammals using the probes corresponding to the mammalian sequence, and are found to range from 6 kb to 2 Mb, depending on the species (82–84). For example, the telomere lengths ranged from 10 to 15 kb in humans (84), 10 kb to 2 Mb in the chicken (*Gallus domesticus*) (82,83), 50 kb in the turtle (*Pseudemys scripta*) (82), 100 kb in the mud puppy (*Necturus maculosus*) (82), 20 kb in the rainbow trout (*Oncorhynchus mykiss*) (82), 6 kb in the sea urchin (*Strongylocentrotus purpuratus*) (82), and 10–50 kb in the African clawed toad (*Xenopus laevis*) (83). In this study, we found that the telomere lengths range from approximately 3.58 ± 0.74 to 11.5 ± 1.98 kb ($p < .001$) in *N. rachovii*. The telomere sequence of *N. rachovii* was not previously known, and our study represents the first use of a mammal's telomere probes to study the telomere length of *N. rachovii* and further confirms that they can be performed in *N. rachovii*.

In this study, we used 1-, 4-, and 7-month-old fish to study the expression of their age-related markers. According to a previous study, the life span of *N. rachovii* is about 8.5 months (24). A 1-month-old fish represents about 12% of life span and may be considered ''young,'' a 4-month-old fish represent about 47% of life span and may be considered ''middle-aged,'' and a 7-month-old fish represent about 82% of life span and may be considered ''old.'' However, the longevity of *N. rachovii* seems to depend on the husbandry conditions (24). Therefore, we cannot definitely define the stages of life simply based on age. Nevertheless, this study shows a definite tendency that the expression of age-related markers is correlated with age.

To know the average value of protein oxidation, lipid peroxidation, enzyme activities, and telomere length in whole fish, we used the body after the removal of the head and internal organs as the source of material to obtain the average values of these age-related markers in *N. rachovii*. However, a previous study showed that telomere lengths in human tissues were decreased in liver, renal cortex, and spleen, but no significant decrease was observed in the cerebral cortex and myocardium (85), suggesting that the aging process is different in individual tissues. Similar studies have been done in guppies (86–88). For example, in the heart, no significant changes were evident until the fish were 3 years old, when a loss of muscle fibers in the ventricles of old fish was noted, with deposition of collagen in the bulbous arteriosus. Whereas histological analysis of the brains throughout the life span showed no overall loss of tissue, in both genders a loss of neurons from the stratum griseum periventriculare in the midbrain roof occurred with age (17). Therefore, extrapolating results from one or two tissues instead of the whole organism should be avoided. By using the body after the removal of the head and internal organs (which includes skin, bones, and red and white muscles), we can obtain an average value of age-related markers on the aging of *N. rachovii*. Nevertheless, a more refined study of a single tissue is required if we wish to know the values of these age-related markers from a single tissue.

Acknowledgments

This work was supported by grant CMRPD 140062 from the Chang Gung Memorial Hospital, Taiwan.

We thank Dr. Hsiu-Chuan Yen for help with CAT, GPX, and SOD assays, Dr. Min-Chi Chen for help with statistical analysis, and Dr. Tzu-Chien Van Wang for help with telomerase activity and telomere length assays.

Correspondence

Address correspondence to Chin-Yuan Hsu, PhD, Department of Life Science, Chang Gung University, 259, Wen-Hwa 1st Road, Kwei-Shan, Tao-Yuan 333, Taiwan. E-mail: hsu@mail.cgu.edu.tw

References

1. Chapman ML, Rubin BR, Gracy RW. Increased carbonyl content of proteins in synovial fluid from patients with rheumatoid arthritis. *J Rheumatol*. 1989;16:15–18.
2. Smith MA, Perry PL, Sayre LM, Anderson VE, Beal MF, Kowal N. Oxidative damage in Alzheimer's disease. *Nature*. 1996;382:120–121.
3. Minamino T, Miyauchi H, Yoshida T, Ishida Y, Yoshida H, Komuro I. Endothelial cell senescence in human atherosclerosis: role of telomere in endothelial dysfunction. *Circulation*. 2002;105:1541–1544.
4. Guarente L, Kenyon C. Genetic pathways that regulate ageing in model organisms. *Nature*. 2000;408:255–262.
5. Johnson TE. Advantages and disadvantages of *Caenorhabditis elegans* for aging research. *Exp Gerontol*. 2003;38:1329–1332.
6. Katic M, Kahn CR. The role of insulin and IGF-1 signaling in longevity. *Cell Mol Life Sci*. 2005;62:320–343.
7. Gerhard G, Kauffman E, Wang X, et al. Life spans and senescent phenotypes in two strains of zebrafish (*Danio rerio*). *Exp Gerontol*. 2002;37:1055–1068.

8. Gerhard GS. Comparative aspects of zebrafish (*Danio rerio*) as a model for aging research. *Exp Gerontol*. 2003;38:1333–1341.
9. Kishi S, Uchiyama J, Baughman A, Goto T, Lin M, Tsai S. The zebrafish as a vertebrate model of functional aging and very gradual senescence. *Exp Gerontol*. 2003;38:777–786.
10. Kishi S. Functional aging and gradual senescence in zebrafish. *Ann N Y Acad Sci*. 2004;19:521–526.
11. Rudolph KL, Chang S, Lee HW, et al. Longevity, stress response, and cancer in aging telomerase-deficient mice. *Cell*. 1999;96:701–712.
12. Hastings R, Li N-C, Lacy PS, et al. Rapid telomere attrition in cardiac tissue of the ageing Wistar rat. *Exp Gerontol*. 2004;39:855–857.
13. Nasir L, Devlin P, McKevitt T, Rutteman G, Argyle DJ. Telomere lengths and telomerase activity in dog tissues: a potential model system to study human telomere and telomerase biology. *Neoplasia*. 2001; 3:351–359.
14. Davis T, Skinner JW, Faragher RG, Jones CJ, Kipling D. Replicative senescence in sheep fibroblasts is a p53 dependent process. *Exp Gerontol*. 2005;40:17–26.
15. Patnaik BK, Mahapatro N, Jena BS. Ageing in fishes. *Gerontology*. 1994;40:113–132.
16. Woodhead AD. Aging, the fishy side: an appreciation of Alex Comfort's studies. *Exp Gerontol*. 1998;33:39–51.
17. Gerhard GS. Small laboratory fish as models for aging research. *Ageing Res Rev*. 2007;6:64–72.
18. Detrich HW III, Westerfield M, Zon LI. Overview of the zebrafish system. *Methods Cell Biol*. 1999;59:3–10.
19. Eisen JS. Zebrafish make a big splash. *Cell*. 1996;87:969–977.
20. Keller ET, Murtha JM. The use of mature zebrafish (*Danio rerio*) as a model for human aging and disease. *Comp Biochem Physiol C Toxicol Pharmacol*. 2004;138:335–341.
21. Liu RK, Walford RL. Increased growth and life-span with lowered ambient temperature in the annual fish, *Cynolebias adloffi*. *Nature*. 1966;212:1277–1278.
22. Matias JR, Markofsky J. The survival of embryos of the annual fish *Nothobranchius guentheri* exposed to temperature extremes and the subsequent effects on embryonic diapause. *J Exp Zool*. 1978;204:219–228.
23. Valdesalici S, Cellerino A. Extremely short lifespan in the annual fish *Nothobranchius furzeri*. *Proc R Soc Lond B Biol Sci*. 2003;270:S189–S191.
24. Herrera M, Jagadeeswaran P. Annual fish as a genetic model for aging. *J Gerontol A Biol Sci Med Sci*. 2004;59A:101–107.
25. Terzibasi E, Valenzano DR, Cellerino A. The short-lived fish *Nothobranchius furzeri* as a new model system for aging studies. *Exp Gerontol*. 2007;42:81–89.
26. Jagadeeswaran P. Response to Cellerino on annual killifishes. *J Gerontol A Biol Sci Med Sci*. 2005;60:1492.
27. Dimri GP, Lee X, Basile G, et al. A biomarker that identifies senescent human cells in culture and in aging skin in vivo. *Proc Natl Acad Sci U S A*. 1995;92:9363–9367.
28. Nakano M, Oenzil F, Mizuno T, Gotoh S. Age-related changes in the lipofuscin accumulation of brain and heart. *Gerontology*. 1995;41: 69–79.
29. Stadtman ER. Protein oxidation and aging. *Science*. 1992;257:1220–1224.
30. Almeida H, Magalhães MC, Magalhães MM. Age-related changes in lipid peroxidation products in rat adrenal gland. *Age*. 1998;21: 119–121.
31. Wei YH, Lee HC. Oxidative stress, mitochondrial DNA mutation, and impairment of antioxidant enzymes in aging. *Exp Biol Med (Maywood)*. 2002;227:671–682.
32. Blander G, de Oliveira RM, Conboy CM, Haigis M, Guarente L. Superoxide dismutase 1 knock-down induces senescence in human fibroblasts. *J Biol Chem*. 2003;278:38966–38969.
33. Wyllie FS, Jones CJ, Skinner JW, et al. Telomerase prevents the accelerated cell ageing of Werner syndrome fibroblasts. *Nat Genet*. 2000;24:16–17.
34. Benetos A, Okuda K, Lajemi M, et al. Telomere length as an indicator of biological aging: the gender effect and relation with pulse pressure and pulse wave velocity. *Hypertension*. 2001;37:381–385.
35. Brunk UT, Terman A. Lipofuscin: mechanisms of age-related accumulation and influence on cell functions. *Free Radic Biol Med*. 2002;33: 611–619.
36. Draper HH, Hadley M. Malondialdehyde determination as index of lipid peroxidation. *Methods Enzymol*. 1990;86:421–431.
37. Okutan H, Ozcelik N, Yilmaz HR, Uz E. Effects of caffeic acid phenethyl ester on lipid peroxidation and antioxidant enzymes in diabetic rat heart. *Clin Biochem*. 2005;38:191–196.
38. Lowry OH, Rosebrough NJ, Farr AL, Randall RJ. Protein measurement with the Folin phenol reagent. *J Biol Chem*. 1951;193:265–275.
39. Levine RL, Williams JA, Stadtman ER, Schacter E. Carbonyl assays for determination of oxidatively modified proteins. *Methods Enzymol*. 1994;233:346–357.
40. Sohal RS, Agarwal S, Dubey A, Orr WC. Protein oxidative damage is associated with life expectancy of houseflies. *Proc Natl Acad Sci U S A*. 1993;90:7255–7259.
41. Yen H-C, Chang H-M, Majima HJ, Chen F-Y, Li S-H. Levels of reactive oxygen species and primary antioxidant enzymes in WI38 versus transformed WI38 cells following bleomcyin treatment. *Free Radic Biol Med*. 2005;38:950–959.
42. Yen H-C, Chen B-S, Hsu Y-T. Effect of anticoagulants and storage of coupling reagent on the activity assay of extracellular glutathione peroxidase in human plasma. *J Biomed Lab Sci*. 2004;16:6–10.
43. Spitz DR, Oberley LW. An assay for superoxide dismutase activity in mammalian tissue homogenates. *Anal Biochem*. 1989;179:8–18.
44. Kim NW, Wu F. Advances in quantification and characterization of telomerase activity by the telomeric repeat amplification protocol (TRAP). *Nucleic Acids Res*. 1997;25:2595–2597.
45. Argyle D, Ellsmore V, Gault EA, Munro AF, Nasir L. Equine telomeres and telomerase in cellular immortalisation and ageing. *Mech Ageing Dev*. 2003;124:759–764.
46. Kurz DJ, Decary S, Hong Y, Erusalimsky JD. Senescence-associated β-galactosidase reflects an increase in lysosomal mass during replicative ageing of human endothelial cells. *J Cell Sci*. 2000;113:3613–3622.
47. Genade T, Benedetti M, Terzibasi E, et al. Annual fishes of the genus *Nothobranchius* as a model system for aging research. *Aging Cell*. 2005;4:223–233.
48. Valenzano DR, Terzibasi E, Genade T, Cattaneo A, Domenici L. Resveratrol prolongs lifespan and retards the onset of age-related markers in a short-lived vertebrate. *Curr Biol*. 2006;16:296–300.
49. Terman A, Brunk UT. Lipofuscin. *Int JBiochem Cell Biol*. 2004; 36:1400–1404.
50. Reichel W. Lipofuscin pigment accumulation and distribution in five rat organs as a function of age. *J Gerontol*. 1968;23:145–153.
51. Oliver CN, Ahn B-W, Moerman EJ, Goldstein S, Stadtman ER. Age-related changes in oxidized proteins. *J Biol Chem*. 1987;262: 5488–5491.
52. Welis-Knecht MC, Huggins TG, Dyer G, Thorpe SR, Baynes JW. Oxidized amino acids in lens protein with age. *J Biol Chem*. 1993;268: 12348–12352.
53. Levine RL, Garland D, Oliver CN, et al. Determination of carbonyl content in oxidatively modified proteins. *Methods Enzymol*. 1990; 186:464–478.
54. Aldini G, Dalle-Donne I, Facino RM, Milzani A, Carini M. Intervention strategies to inhibit protein carbonylation by lipoxidation-derived reactive carbonyls. *Med Res Rev*. 2007;27:817–868.
55. Esterbauer H, Schaur RJ, Zollner H. Chemistry and biochemistry of 4-hydroxynonenal, malonaldehyde and related aldehydes. *Free Radic Biol Med*. 1991;11:81–128.
56. Draper HH, McGirr LG, Hadley M. The metabolism of malondialdehyde. *Lipids*. 1986;21:305–307.
57. Yuan Q, Zhu X, Sayre LM. Chemical nature of stochastic generation of protein-based carbonyls: metal-catalyzed oxidation versus modification by products of lipid oxidation. *Chem Res Toxicol*. 2007;20:129–139.
58. Terman A, Brunk UT. On the degradability and exocytosis of ceroid/lipofuscin in cultured rat cardiac myocytes. *Mech Ageing Dev*. 1998; 100:145–156.
59. Terman A, Brunk UT. Ceroid/lipofuscin formation in cultured human fibroblasts: the role of oxidative stress and lysosomal proteolysis. *Mech Ageing Dev*. 1998;104:277–291.
60. Ozawa T. Genetic and functional changes in mitochondria associated with aging. *Physiol Rev*. 1997;77:425–464.
61. Richter C. Oxidative damage to mitochondrial DNA and its relationship to ageing. *Int J Biochem Cell Biol*. 1995;27:647–653.
62. Sitte N, Merker M, von Zglinicki T, Grune T, Davies KJA. Protein oxidation and degradation during cellular senescence of human BJ

fibroblasts: part I-effects of proliferative senescence. *FASEB J*. 2000;14:2495–2502.
63. Sitte N, Merker M, von Zglinicki T, Davies KJA, Grune T. Protein oxidation and degradation during cellular senescence of human BJ fibroblasts: part II-aging of nondividing cells. *FASEB J*. 2000;14:2503–2510.
64. Halliwell B, Gutteridge JMC. *Free radicals in biology and medicine*. New York: Oxford University Press; 1999.
65. Semsei I, Kao G, Richardson A. Expression of superoxide dismutase and catalase in rat brain as function of age. *Mech Ageing Dev*. 1991;58:13–19.
66. Gupta A, Hasan M, Chander R, Kapoor NK. Age-related elevation of lipid peroxidation products: diminution of superoxide dismutase activity in the central nervous systems of rats. *Gerontology*. 1991;37:305–309.
67. Siqueira IR, Fochesatto C, de Andrade A, et al. Total antioxidant capacity is impaired in different structures from aged rat brain. *Int J Dev Neurosci*. 2005;23:663–671.
68. Zhu Y, Cavey PM, Ling Z. Age-related changes in glutathione and glutathione-related enzymes in rat brain. *Brain Res*. 2006;1090:35–44.
69. Kishido T, Unno K, Yoshida H, et al. Decline in glutathione peroxidase activity is a reason for brain senescence: consumption of green tea catechin prevents the decline in its activity and protein oxidative damage in ageing mouse brain. *Biogerontology*. 2007;8:423–430.
70. Brunk UT, Terman A. The mitochondrial-lysosomal axis theory of aging–Accumulation of damaged mitochondria as a result of imperfect autophagocytosis. *Eur J Biochem*. 2002;269:1996–2002.
71. Massimo CD, Scarpelli P, Lorenzo ND, Caimi G, di Orio F, Ciancarelli MGT. Impaired plasma nitric oxide availability and extracellular superoxide dismutase activity in healthy humans with advancing age. *Life Sci*. 2006;78:1163–1167.
72. Li M, Chiu J-F, Mossman BT, Fukagawa NK. Down-regulation of manganese-superoxide dismutase through phosphorylation of FOXO3a by Akt in explanted vascular smooth muscle cells from old rats. *J Biol Chem*. 2006;281:40429–40439.
73. Morin GB. The human telomere terminal transferase enzyme is a ribonucleoprotein that synthesizes TTAGGG repeats. *Cell*. 1989;59:521–529.
74. Wright WE, Piatysek MA, Rainey WE, Byrd W, Shay JW. Telomerase activity in human germline and embryonic tissues and cells. *Dev Genet*. 1996;18:173–179.
75. Bradford CS, Miller AE, Toumadje A, Nishiyama K, Shirahata S, Barnes DW. Characterization of cell cultures derived from *Fugu*, the Japanese pufferfish. *Mol Mar Biol Biotechnol*. 1997;6:279–288.
76. Yap WH, Yeoh E, Brenner S, Venkatesh B. Cloning and expression of the reverse transcriptase component of pufferfish (*Fugu rubripes*) telomerase. *Gene*. 2005;353:207–217.
77. Yu RM, Chen EX, Kong RY, Ng PK, Mok HO, Au DW. Hypoxia induces telomerase reverse transcriptase (TERT) gene expression in non-tumor fish tissues in vivo: the marine medaka (*Oryzias melastigma*) model. *BMC Mol Biol*. 2006;7:27 doi:10.1186/1471-2199-7-27.
78. Moyzis RK, Buckingham JM, Cram LS, et al. A highly conserved repetitive DNA sequence, (TTAGGG)n, present at the telomeres of human chromosomes. *Proc Natl Acad Sci U S A*. 1988;85:6622–6626.
79. Harley CB, Futcher AB, Greider CW. Telomeres shorten during ageing of human fibroblasts. *Nature*. 1990;345:458–460.
80. Kipling D. Telomeres, replicative senescence and human ageing. *Maturitas*. 2001;38:25–37.
81. Lindsey J, McGill NI, Lindsey LA, Green DK, Cooke HJ. In vivo loss of telomeric repeats with age in humans. *Mutat Res*. 1991;256:45–48.
82. Lejnine S, Makarov VL, Langmore JP. Conserved nucleoprotein structure at the ends of vertebrate and invertebrate chromosomes. *Proc Natl Acad Sci U S A*. 1995;92:2393–2397.
83. Delany ME, Daniels LM, Swanberg SE, Taylor HA. Telomeres in the chicken: genome stability and chromosome ends. *Poult Sci*. 2003; 82:917–926.
84. Davis T, Kipling D. Telomeres and telomerase biology in vertebrates: progress towards a non-human model for replicative senescence and ageing. *Biogerontology*. 2005;6:371–385.
85. Takubo K, Izumiyama-Shimomura N, Honma N, et al. Telomere lengths are characteristic in each human individual. *Exp Gerontol*. 2002;37:523–531.
86. Woodhead AD. Fish in studies of aging. *Exp Gerontol*. 1978;13: 125–140.
87. Woodhead AD, Pond V. Aging changes in the optic tectum of the guppy Poecilia (Lebistes) reticulates. *Exp Gerontol*. 1984;19:305–311.
88. Woodhead AD, Pond V, Dailey K. Aging changes in the kidneys of two poeciliid fishes, the guppy *Poecilia reticulatus* and the Amazon molly P. formosa. *Exp Gerontol*. 1983;18:211–221.

Received February 18, 2008
Accepted July 22, 2008
Decision Editor: Huber R. Warner, PhD